Electron bunch train excited higher-order modes in a superconducting RF cavity [*]

Yong-Feng Gao(高永凤)   Sen-Lin Huang(黄森林)[1)]   Fang Wang(王芳)   Li-Wen Feng(冯立文)

De-Hao Zhuang(庄德浩)   Lin Lin(林林)   Feng Zhu(朱凤)   Jian-Kui Hao(郝建奎)

Sheng-Wen Quan(全胜文)   Ke-Xin Liu(刘克新)

Institute of Heavy Ion Physics and State Key Laboratory of Nuclear Physics and Technology, School of Physics,
Peking University, Beijing 100871, China

Abstract: Higher-order mode (HOM) based intra-cavity beam diagnostics has been proved effective and convenient in superconducting radio-frequency (SRF) accelerators. Our recent research shows that the beam harmonics in the bunch train excited HOM spectrum, which have much higher signal-to-noise ratio than the intrinsic HOM peaks, may also be useful for beam diagnostics. In this paper, we will present our study on bunch train excited HOMs, including a theoretical model and recent experiments carried out based on the DC-SRF photoinjector and SRF linac at Peking University.

Keywords: HOMs, bunch train, SRF cavity, beam diagnostics

PACS: 29.20.Ej   **DOI:** 10.1088/1674-1137/41/4/047002

1   Introduction

Higher-order modes (HOMs) are excited when an electron beam passes through a radio-frequency (rf) cavity. This is one of the main causes of emittance dilution [1] and beam current limit in a superconducting rf (SRF) cavity [2–4]. For a TESLA cavity, two coaxial type couplers are therefore installed on both ends of the cavity with a specific orientation to extract HOMs and transfer the power to the load [5].

A HOM signal contains beam information, such as the beam position in the rf cavity, the beam arrival time, etc [6]. It can be directly used for beam diagnostics without additional vacuum instruments. Such HOM-based beam diagnostics is convenient and cheap, and more importantly, it can provide local beam information in a cryomodule. Many laboratories have conducted studies on HOM-based beam diagnostics. At JAEA, the HOM signal excited by a macro pulse was detected to obtain beam position information [7]. At DESY, a dipole mode signal excited by a single bunch was applied for SRF cavity alignment and beam position measurements [8–11].

In the spectrum of a HOM signal excited by multiple bunches, two kinds of peak exist: intrinsic HOM peaks and beam harmonics [12, 13]. This can be observed clearly when the bunch repetition rate is high enough that the beam harmonics can be identified by

equipment. Under proper conditions, the beam harmonics are much stronger than the intrinsic HOM peaks, so they may provide a useful means to obtain beam information with high signal-to-noise ratio. In this paper, we will first present our theoretical model for bunch train excited HOMs and then the measurement results on a DC-SRF photoinjector and SRF linac. We will also report our recent tests of beam diagnostics on the DC-SRF photoinjector.

2   Electron bunch train excited HOMs

When a relativistic electron beam passes through an SRF cavity, it will excite HOMs. The HOM voltage can be calculated as

$$V_{\mathrm{b}}(t) = \sum_m \int_{-\infty}^{t} V_m(t-\tau)\rho_{\mathrm{b}}(\tau)\mathrm{d}\tau, \qquad (1)$$

where the summation represents the voltage superposition of all HOMs excited in the SRF cavity, V_m is the single electron induced voltage signal of the mth HOM ($m = 1,2,3,...$), $\rho_{\mathrm{b}} = I_{\mathrm{b}}/e$, I_{b} is the current signal of electron beam and e is the charge of an electron. Changing variable from τ to $\tau' = t-\tau$, we have

$$V_{\mathrm{b}}(t) = \sum_m \int_0^{\infty} V_m(\tau')\rho_{\mathrm{b}}(t-\tau')\mathrm{d}\tau'. \qquad (2)$$

The HOM spectrum is a Fourier transform of the HOM voltage, whose amplitude, the HOM magnitude spectrum, can be derived as

$$V_{\rm b}(f) = |\hat{\rho}_{\rm b}(f)| \cdot \left| \sum_m \int_0^\infty V_m(\tau') {\rm e}^{-2\pi i f \tau'} {\rm d}\tau' \right|, \quad (3)$$

where

$$\hat{\rho}_{\rm b} = \int_{-\infty}^\infty \rho_{\rm b}(t) {\rm e}^{-2\pi i f t} {\rm d}t. \quad (4)$$

Considering the HOM wakefield excited by a single electron exists only when $\tau' > 0$, the lower limit of integration in Eq. (3) can be extended to $-\infty$ and as a result,

$$V_{\rm b}(f) = |\hat{\rho}_{\rm b}(f)| \cdot \left| \sum_m \hat{V}_m(f) \right|, \quad (5)$$

in which

$$\hat{V}_m(f) = \int_{-\infty}^\infty V_m(\tau') {\rm e}^{-2\pi i f \tau'} {\rm d}\tau' \quad (6)$$

is the single electron excited HOM spectrum. Referring to, e.g., [14, 15], it can be calculated as

$$\hat{V}_m(f) = e \alpha_m Z_m^\parallel(f), \quad (7)$$

in which α_m is the mode excitation factor of the $m^{\rm th}$ HOM, accounting for the coupling efficiency between the HOM field and electron energy. For dipole mode [16], e.g., α_m accounts for the coupling efficiency due to the transverse offset of electron beam trajectory in the SRF cavity. $Z_m^\parallel(f)$ in the equation is the longitudinal impedance of the $m^{\rm th}$ HOM, which can often be modelled by an equivalent parallel LRC resonator circuit and given by [14]

$$Z_m^\parallel(f) = \frac{(R/Q)_m}{1/Q_m + i(f_m/f - f/f_m)}, \quad (8)$$

where Q_m and f_m are the quality factor and eigenfrequency of the $m^{\rm th}$ HOM, respectively.

Plugging Eqs. (7) and (8) into Eq. (5), the HOM magnitude spectrum can be calculated as

$$V_{\rm b}(f) = I_{\rm b}(f) \cdot \left| \sum_m \frac{\alpha_m (R/Q)_m}{1/Q_m + i(f_m/f - f/f_m)} \right|, \quad (9)$$

in which $I_{\rm b}(f) = |\hat{I}_{\rm b}(f)|$, and

$$\hat{I}_{\rm b}(f) = e \hat{\rho}_{\rm b}(f) = \int_{-\infty}^\infty I_{\rm b}(t) {\rm e}^{-2\pi i f t} {\rm d}t \quad (10)$$

is the current spectrum of the electron beam. Introducing $\delta f_m = f - f_m$, we have

$$V_{\rm b}(f) = I_{\rm b}(f) \cdot \left| \sum_m \frac{\alpha_m (R/Q)_m}{1/Q_m - i \left(\dfrac{\delta f_m}{f_m + \delta f_m} + \dfrac{\delta f_m}{f_m} \right)} \right|. \quad (11)$$

The equation can be approximated as

$$V_{\rm b}(f) = \left| \sum_m \alpha_m I_{\rm b}(f) \cdot \frac{f_m}{2\delta f_m} (R/Q)_m \right|, \quad (12)$$

when $1 \gg \delta f_m / f_m \gg 1/Q_m$.

To calculate the current magnitude spectrum, $I_{\rm b}(f)$ in Eq. (9), we consider the electron beam to be comprised of a train of electron bunches with the same current profiles and equally separated by $T_{\rm b}$ in the time domain. The current signal can be expressed as the convolution of the single bunch current profile and a comb function, i.e.,

$$I_{\rm b}(t) = \sum_{n=0}^{N-1} \int_{-\infty}^\infty I_1(\tau) \delta(t - nT_{\rm b} - \tau) {\rm d}\tau, \quad (13)$$

where N is the number of bunches in the train, $I_1(t)$ represents the current profile of a single bunch, and $\delta(t)$ is the Dirac Delta function. The corresponding current spectrum is the product of Fourier transforms of $I_1(t)$ and the comb function. It is easy to obtain the amplitude of the current spectrum as

$$I_{\rm b}(f) = \left| \frac{\sin(\pi N f T_{\rm b})}{\sin(\pi f T_{\rm b})} \right| \cdot I_1(f), \quad (14)$$

in which $I_1(f) = |\hat{I}_1(f)|$, and

$$\hat{I}_1(f) = \int_{-\infty}^\infty I_1(t) {\rm e}^{-2\pi i f t} {\rm d}t \quad (15)$$

is the Fourier transform of $I_1(t)$. In the case of electron bunch length $\sigma_{\rm t} \ll 1/f_{\rm n}$, $I_1(f)$ can be treated as a constant.

As an example, a typical spectrum of HOM excited by a picosecond electron bunch train was calculated using Eq. (9) and Eq. (14). To clearly illustrate the characteristic of bunch train excited HOMs, only one HOM is considered in the calculation. The parameters are taken according to our experiments as follows: the HOM has an eigenfrequency of 1.7513 GHz and a quality factor of 5×10^5, while the electron beam has a pulse repetition rate ($f_{\rm b} = 1/T_{\rm b}$) of 0.797 MHz and a macro-pulse length of 3 ms.

Figures 1-3 show the calculation results, including the HOM spectrum excited by a single electron, the current spectrum of the bunch train, and the bunch train excited HOM spectrum. It can be seen from Fig. 3 that besides the intrinsic HOM peak (referred to as "intrinsic HOM peak" hereafter), many spectral peaks (lines) at beam harmonic frequencies (referred to as "beam harmonics" hereafter) exist. Moreover, the beam harmonic closest to the intrinsic HOM peak has a much larger amplitude than the intrinsic HOM peak.

The HOM spectrum excited by a single electron shown in Fig. 1 is essentially the SRF cavity's spectral response function to an rf source, while the electron beam plays the role of an rf source with the spectrum shown in Fig. 2. Although the SRF cavity's spectral response function has a very sharp spike at the HOM's eigenfrequency and the ratio between the amplitudes at eigenfrequency and beam harmonics is significant, the rf source, however, has an even higher ratio between the amplitudes at beam harmonics and eigenfrequency. Therefore, many beam harmonics higher than the intrinsic HOM peak can be observed. Obviously, the beam harmonic closest to the intrinsic HOM peak has the maximum amplitude, which can also be inferred from Eq. (12) directly.

It is straightforward to infer that, in the case of only one HOM, the amplitude of beam harmonics has a linear dependency on the coupling efficiency α_m between the HOM field and electron energy. When the HOM
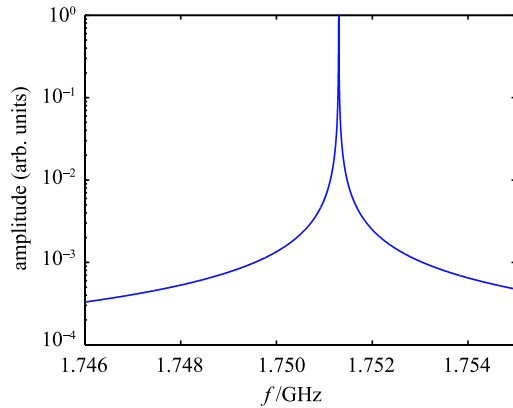

Fig. 1.   HOM spectrum excited by a single electron (calculation result). In the calculation, only one HOM is considered, which has an eigenfrequency of 1.7513 GHz and a quality factor of 5×10^5.
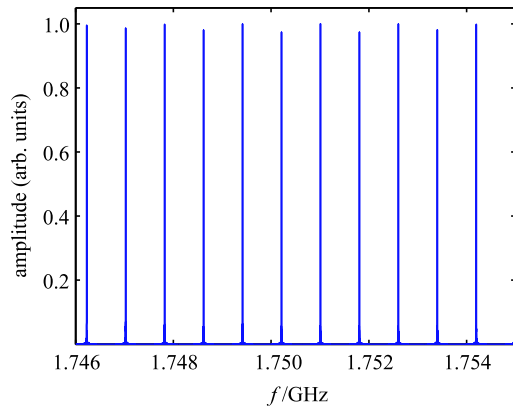

Fig. 2.   Current spectrum of a train of electron bunches (calculation result). In the calculation, the electron beam has a pulse repetition rate of 0.797 MHz and a macro-pulse length of 3 ms.
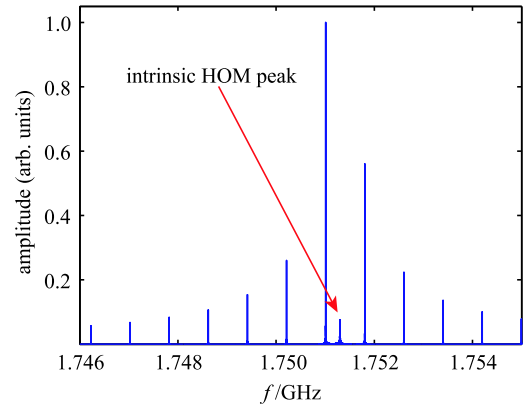

Fig. 3.   Bunch train excited HOM spectrum (calculation result). In the calculation, only one HOM is considered, which has an eigenfrequency of 1.7513 GHz and a quality factor of 5×10^5. The electron beam has a pulse repetition rate of 0.797 MHz and a macro-pulse length of 3 ms.

is a dipole mode, the beam harmonic amplitude is inevitably proportional to the beam offset and therefore it can provide the beam position information, as that can be provided by the intrinsic HOM excited by a single electron bunch. Compared to the latter case, the beam harmonic has a much higher amplitude, which can provide a much higher signal-to-noise ratio, especially when the HOM quality factor Q_m is small.

In practice, multiple HOMs could be excited in the SRF cavity. One can infer from Eq. (12) and Eq. (14) that different HOMs would contribute to the same beam harmonic. However, the main contribution comes from the mode with higher R/Q and with the eigenfrequency near the beam harmonics. With a properly chosen HOM, which has an eigenfrequency close to the beam harmonics and an R/Q much higher than neighboring HOMs, the contributions from other HOMs can be ignored and the above discussion for only one HOM is still valid. Under such a condition, it is obvious that the beam harmonics can be used for beam diagnostics.

3   HOM experiments on the DC-SRF photoinjector

Preliminary experiments have been carried out based on the DC-SRF photoinjector at Peking University. The DC-SRF photoinjector comprises a pair of DC Pierce electrodes and a 3.5-cell 1.3 GHz TESLA-type cavity [17]. It has been in operation since 2014 and can deliver 3–5 MeV, 6–50 pC electron bunches with a bunch length of approximately 5 ps and repetition rate tunable between 162.5 kHz and 81.25 MHz [18, 19]. In the DC-SRF photoinjector, the electron bunches emitted from

the photocathode are first accelerated by the DC Pierce structure to 50-90 keV. After a drift section of approximately 17 mm, the bunches enter the 3.5-cell SRF cavity. They are soon accelerated to β close to 1 in the first half cell. Therefore, the effect of β variation on the electron beam excited HOM [20] can be ignored in our experiments.

The HOM experiments were performed when the DC-SRF photoinjector was operated in pulse mode with a macro pulse length of a few milliseconds. The electron beam excited HOM signal in the 3.5-cell SRF cavity was extracted from the pickup port of the cavity and then amplified by a three-stage power amplifier, which had a gain of 30 dB over the frequency range from 1.0 GHz to 2.4 GHz, before being delivered to the spectrum analyzer. Figure 4 shows an example of the measured HOM spectrum, in which the electron beam has a bunch repetition rate of 0.797 MHz and a macro pulse length of 3 ms. In the measurement, the spectrum analyzer was set to sweep across the frequency range from 1.746 to 1.755 GHz, in which the TE_{111} $3\pi/4$ mode, whose R/Q is the highest among the neighboring HOMs in the SRF cavity [21], is expected.
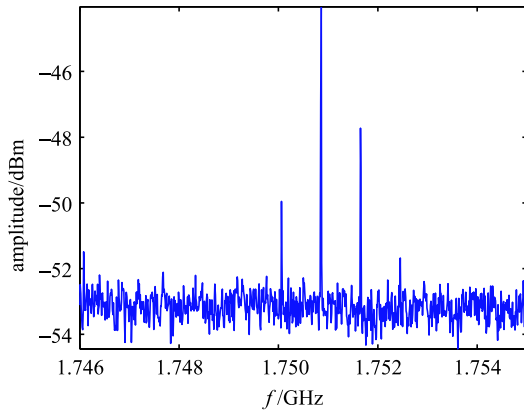

Fig. 4.   Measured electron beam excited HOM spectrum in the 3.5-cell cavity of the DC-SRF photoinjector. In the measurement, the electron beam has a pulse repetition rate of 0.797 MHz and a macro-pulse length of 3 ms.

The result is consistent with that obtained in analytical calculation (see Fig. 3). In Fig. 4, four discrete spectral lines equally spaced by 0.797 MHz can be clearly observed, corresponding to beam harmonics. The intrinsic HOM peak, however, is at noise level and cannot be observed. From the figure one can infer that the eigenfrequency of the mode is between 1.7509 and 1.7516 GHz, corresponding to the frequencies of the two highest beam harmonics, respectively.

It is worth pointing out that, according to rf calculation [21], the R/Q of the TE_{111} $3\pi/4$ mode is 3 - 4 times that of the closest HOMs, the TE_{111} $\pi/2$ mode and

TM_{110} π mode. These two HOMs have an eigenfrequency of 1.687 GHz and 1.795 GHz (rf measurement results, see [21]), respectively. The differences (δf_m) between the eigenfrequencies and the highest beam harmonic frequency (~ 1.751 GHz) are 64 MHz and 44 MHz accordingly, which are at least 55 times the frequency difference between the TE_{111} $3\pi/4$ mode and the beam harmonic (< 0.797 MHz). According to Eq. (12), the contributions of the TE_{111} $\pi/2$ mode and TM_{110} π mode to the highest beam harmonic are approximately 200 times lower than that of the TE_{111} $3\pi/4$ mode, and therefore can be ignored.

Among the HOMs, dipole modes are related to beam position in the SRF cavity. Therefore, preliminary investigation on the relationship between electron beam position and dipole modes was carried out. Three sets of tests were performed, in which the TE_{111} $3\pi/4$, TM_{110} π, and TM_{110} $\pi/4$ modes, which have the highest R/Q among all dipole modes, were measured. The electron bunch repetition rate was set to be 0.797 MHz for TE_{111} $3\pi/4$ mode measurement and 0.406 MHz for TM_{110} π mode and TM_{110} $\pi/4$ mode measurements.

In all the three measurements, the beam harmonics with the largest amplitude were chosen for analysis. Their frequencies are 1.7509 GHz (for TE_{111} $3\pi/4$ mode), 1.8013 GHz (for TM_{110} π mode), and 1.8875 GHz (for TM_{110} $\pi/4$ mode), respectively. The electron beam position in the SRF cavity was scanned by adjusting the position of the drive laser [22] spot on the photocathode. The whole scanning range of the electron beam position is estimated to be 8 mm. The measured beam harmonic amplitudes, scaled by the electron beam current, are plotted as a function of the electron beam position in Fig. 5. We need to point out that, although the drive
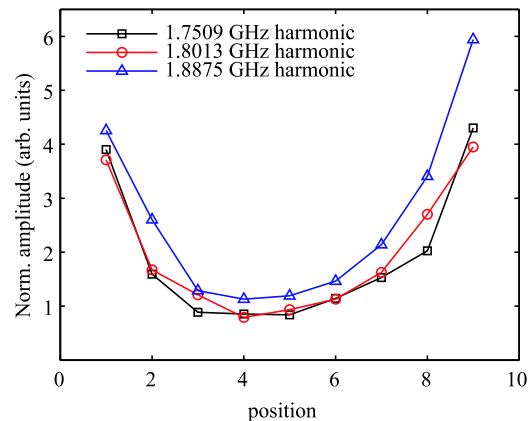

Fig. 5.   Measured electron beam excited HOM signal (beam harmonic) amplitude as a function of the electron beam position in the 3.5-cell SRF cavity of the DC-SRF photoinjector. Position number is used instead of the real position of the electron beam in the 3.5-cell cavity since the absolute position has not been calibrated.

laser position on the photocathode can be determined experimentally, the beam position in the SRF cavity is difficult to precise calibrate at the moment. Therefore, the point numbers of the scan are used in Fig. 5 to represent different beam positions.

From Fig. 5, in all three sets of tests, the beam harmonic amplitude has its minimum value between positions 4 and 5, which can be considered as the cavity center, and it grows when the electron beam deviates from the cavity center. This proves that the beam harmonics can be used for beam position measurement.

4   HOM signal from a 9-cell SRF cavity

Recently an SRF linac designed by Peking University was brought into operation to further accelerate the electron beam from the DC-SRF photoinjector. The linac [23] consists of two 1.3-GHz 9-cell TESLA-type cavities. At either side of the 9-cell cavities two HOM couplers are mounted with an azimuth angle of $115°$. The HOM signal in the 9-cell SRF cavity can be extracted from the HOM coupler.

Spectrum measurements of the bunch train excited HOMs have been carried out based on the SRF linac. Similar to the above DC-SRF experiments, the linac was operated in pulse mode with a macro pulse length of a few milliseconds. Figure 6 shows a measured spectrum, where the spectrum analyzer was set to sweep across the frequency range around the TE_{111} π mode. Both the beam harmonic and the intrinsic HOM peak can be observed, and the beam harmonic has a much higher (five orders of magnitude) amplitude and a much narrower band. During the experiment, we also observed that the intrinsic HOM peak drifted randomly, which might be attributed to the cavity vibration, while the beam harmonic kept unchanged. This indicates that beam har-

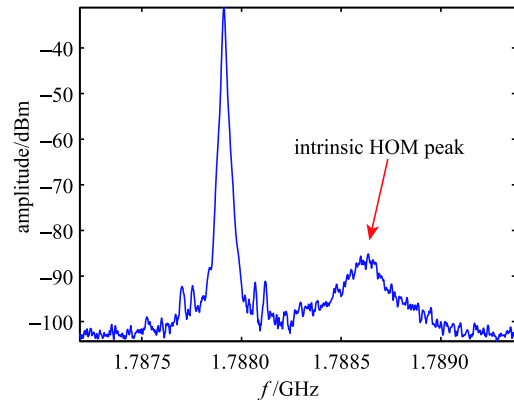monics have an advantage in those applications requiring stable HOM spectral performance.

Fig. 6.   Measured spectrum of electron beam excited HOM signal extracted from the HOM coupler. In the measurement, the electron beam has a pulse repetition rate of 27 MHz and a macropulse length of 3 ms.

5   Conclusion

In this paper we have presented our study on bunch train excited HOMs in an SRF cavity. Compared to the HOMs excited by a single electron bunch, the bunch train excited HOMs have distinct spectral features, which has been shown both theoretically and experimentally. Under proper conditions, beam harmonics are much stronger than the intrinsic HOM peaks. Therefore the beam harmonics could provide a useful means to obtain electron beam information with high signal-to-noise ratio. Preliminary experiments demonstrate the use of dipole mode beam harmonics in electron beam position diagnostics in the SRF cavity. Further research on HOM-based beam diagnostics will be carried out.

References

1   A. Vostrikov et al, Physics Procedia, **79**: 46–53 (2015)
2   R. Calaga et al, in Proceedings SRF2003 (Travemunde/Lubeck, Germany: JACoW, 2003), p. 282
3   S. Chen et al, Chinese Physics C, **37**: 087001 (2013)
4   S. Chen et al, Chinese Physics C, **39**: 017006 (2015)
5   J. Sekutowicz, in Proceedings of SRF93 (Newport News, VA, USA: JACoW, 1993), p. 426
6   J. Frisch et al, SLAC-PUB-12161 (2006)
7   M. Sawamura, in Proceedings of PAC07 (Albuquerque, NM, USA: JACoW, 2007), p. 4060
8   P. Zhang et al, arXiv: 1208.2122v1 (2012)
9   L. Shi et al, Physics Procedia, **77**: 42–49 (2015)
10   S. Molloy et al, Meas. Sci. Technol., **18**: 2314 (2007)
11   N. Baboi et al, in Proceedings of the SRF2011 (Chicago, IL, USA: JACoW, 2011), p. 239
12   S.I. Kurokawa et al, Beam Measurement (World Scientific Publishing Co. Pte. Ltd, 1999), p. 67–77
13   S. Kim, et al, Nucl. Instrum. and Methods A, **492**: 1–10 (2002)
14   A.W. Chao, *Physics of Collective Beam Instabilities in High Energy Accelerators* (John Wiley & Sons, Inc, 1993), p. 248–250
15   A. Novokhatski, SLAC-PUB-10792 (2004)
16   H. Padamsee, J. Knobloch, and T. Hays, RF Superconductivity for Accelerators (John Wiley & Sons, Inc, 1998), p. 340–342
17   S.W. Quan et al, Phys. Rev. ST Accel. Beams, 13: 042001 (2010)
18   S.W. Quan et al, Nucl. Instrum. Methods Phys. Res. A, **798**: 117 (2015)
19   X. Wen et al., Nucl. Instrum. Methods Phys. Res. A, **820**: 75 (2016)
20   S.S. Kurennoy, Phys. Rev. ST Accel. Beams, 2: 032001 (1999)
21   Y. Gao, in Proceedings of IPAC2015 (Richmond, VA, USA: JACoW, 2015), p. 965
22   Z.W. Wang et al, Chinese Physics C, **40**: 017004 (2016)
23   F. Zhu et al, in Proceedings of SRF2015 (Whistler, BC, Canada: JACoW, 2015), p. 1443